MNRAS **000**, 1–5 (2019) Preprint 7 January 2020 Compiled using MNRAS LaTeX style file v3.0

# Waveforms from Hierarchical Triples for LISA

Kimpson,[1★] Huan Yang ,[2]
[1] *Mullard Space Science Laboratory, University College London. Holmbury St. Mary, Dorking, Surrey, RH5 6NT, UK,*
[2] *PI, Canada, etc*

Accepted XXX. Received YYY; in original form ZZZ

**ABSTRACT**
blah blah blah

**Key words:** gravitation – pulsars – black hole physics

## 1 INTRODUCTION

Intro...
What are the waveforms from ~ stellar mass BH binaries in hierarchical triple systems, as detected by LISA. Especially those which retain significant eccentricities.

## 2 WAVEFORM MODEL

We now discuss how to construct a waveform model for gravitational waves from BH binaries in the LISA band...

### 2.1 Equations of motion

In specifying the equation of motion of the inner binary we adopt the formalism of (Randall & Xianyu 2018). Within this framework the evolution of the orbital elements has contributions from the Kozai-Lidov mechanism in addition to the usual PN precession of periastron and relativistic corrections due to the emission of gravitational radiation. In order to properly model the waveforms from astrophysical HT systems across a general parameter space, it is important to consider the convolution of both the KL and GW radiative effects. Whilst for specific configurations the KL effects can dominate over the GW ones, more generally the GW effects act to dampen the impact of KL oscillations. To construct a general, accurate model to explore the impact of KL oscillations on the resultant waveform requires a consistent approach to modelling both these effects.

The KL, GW and PN effects imprint on the evolution of 4 key variables of the inner binary: the eccentricity $e$, the semi-major axis $a$, the pericentre angle $\gamma$ and the orbital angular momentum $J$. The complete set of coupled ODEs for the evolution of the orbital parameters are (Randall & Xianyu 2018),

$$\dot{e} = \dot{e}_{\rm KL} + \dot{e}_{\rm GW} \tag{1}$$

$$\dot{\gamma} = \dot{\gamma}_{\rm KL} + \dot{\gamma}_{\rm PN} \tag{2}$$

$$\dot{a} = \dot{a}_{\rm GW} \tag{3}$$

$$\dot{J} = \dot{J}_{\rm GW} \tag{4}$$

where the eccentricity components are

$$\dot{e}_{\rm KL} = \frac{\mathcal{A} a^2 e u(e)}{J} \sin 2\gamma \tag{5}$$

$$\dot{e}_{\rm GW} = \frac{19}{12} C a^{-4} g(e) \tag{6}$$

the $\gamma$-components:

$$\dot{\gamma}_{\rm KL} = 2Ka^2 \left[ \frac{1}{J_1} \left( 2u(e) - 5\sin^2\gamma_1 \left( u(e) - \cos^2 I \right) \right) \right. \tag{7}$$

$$\left. + \frac{\cos I}{J_2} \left( u(e) + 5e_1^2 \sin^2 \gamma_1 \right) \right] \tag{8}$$

$$\dot{\gamma}_{\rm PN} = \lambda a^{-2.5} u^{-1} \tag{9}$$

the evolution of $a$:

$$\dot{a}_{\rm GW} = C a^{-3} u(e)^{-7/2} f(e) \tag{10}$$

and of the angular momentum:

$$\dot{J} = \eta a^{-7/2} (1-e^2)^{-2} h(e) \tag{11}$$

The constants are defined as:

$$C = -64 G^3 \mu m^2 / 5c^5 \tag{12}$$

$$\mathcal{A} = 5K \left( 1 - \cos^2 I \right) \tag{13}$$

$$\lambda = 3/c^2 (Gm)^{3/2} \tag{14}$$

$$K = \frac{3Gm_0 m_1 m_2}{8M} \frac{1}{a_2^3 \left(1 - e_2^2\right)^{3/2}} \tag{15}$$

$$\eta = -\frac{32}{5} \frac{G^{7/2} \mu m^{5/2}}{c^5} \tag{16}$$

whilst the eccentricity functions are given by

$$g(e) = \frac{e}{(1-e^2)^{5/2}} \left( 1 + \frac{121}{304} e^2 \right) \tag{17}$$

★ E-mail: tom.kimpson.16@ucl.ac.uk

$$f(e) = \frac{1}{(1-e^2)^{7/2}} \left(1 + \frac{73}{24}e^2 + \frac{37}{96}e^4\right) \tag{18}$$

$$h(e) = 1 + \frac{7}{8}e^2 \tag{19}$$

$$u(e) = 1 - e^2 \tag{20}$$

We use the subscripts 2 denote variables which relate to the outer binary, and $I$ is the inclination of the inner orbit relative to the outer orbit.

It is possible to solve this set of ODEs numerically to determine the evolution of the binary. However, given the length of the LISA mission ($T \sim 5$ years) and the broad parameter space we wish to explore, it quickly becomes computationally intractable to compute waveforms to sufficient precision in this way. Instead we seek an analytical or semi-analytical approach. Naturally such an method loses something in accuracy compared to the full numerical evolution, but we will show that our approximations which allow an analytical model to be constructed are appropriate and serve to capture the key physics of the systems we wish to investigate. In particular, the characteristic feature of hierarchical triples as distinct from other binaries is the presence of KL oscillations and it is the impact of these on the waveform, in conjunction with other relativistic effects that we wish to model and explore.

### 2.2 Constructing a model

**Why did you propose these parametric solutions?** In constructing a model for the orbital evolution and gravitational waveform we take a semi-analytical approach that proceeds as follows:

(i) For a given system, integrate the equations of motion (Eq. 1 - 4 ) numerically, but coarsely. Whilst numerical, this step is not computationally taxing, taking $< 1s$. This produces a 'training set' of data for the orbital elements.

(ii) Use a non-linear least squares fitting method to fit the training set of $e(t)$ with a parametric solution of the form

$$e(t) = A\sin(\omega t) + B * \cos(\omega t) + \delta \tag{21}$$

(iii) Given $e(t)$ we can solve for $a(t)$ as follows. We can rearrange Eq. 10 to be of the form,

$$a^3 da = C u(e)^{-7/2} f(e) dt \tag{22}$$

The RHS is easily integrable, but the LHS is not given the form of $e(t)$ and $f(e)$ (i.e. Mathematica fails to find a solution). The LHS becomes soluble if we perform a Taylor expansion of $u(e)^{-7/2} f(e)$ about the initial value of the eccentricity. Defining $\xi^N$ as the Taylor expansion to order $N$ of $u(e)^{-7/2} f(e)$, then the time-evolution of the semi-major axis is given as,

$$a(t) = (4C\bar{\xi} + D)^{1/4} \tag{23}$$

where $\bar{\xi} = \int \xi^N dt$, and $D$ is a constant of integration set by the initial conditions. We typically set $N = 12$. The explicit expression for $\xi^{N=12}$ is given in the Appendix.

(iv) From the training set, we can calculate the numerical evolution of $\dot{\gamma}$ via Eq. 2. We can fit $\dot{\gamma}(t)$ again via a non-linear least squares method with a parametric solution of the form,

$$\dot{\gamma}(t) = H + (B_A \sin(B_\omega t + B_C) + B_D)(\sin^2(B_f t + B_g)) \tag{24}$$

which is generally integrable as,

$$\begin{aligned}\gamma(t) = &- \frac{B_A \cos(B_C + t(B_\omega - 2B_f) - 2B_g)}{4(2B_f - B_\omega)} \\ &+ \frac{B_A \cos(B_C + t(B_\omega + 2B_f) + 2B_g)}{4(2B_f + B_\omega)} \\ &+ \frac{1}{2}B_A \left(\frac{\sin(C)\sin(tB_\omega)}{B_\omega} - \frac{\cos(C)\cos(B_\omega t)}{B_\omega}\right) \\ &+ \frac{B_D(B_f t + B_g)}{2B_f} \\ &- \frac{B_D \sin(2(B_f t + B_g))}{4B_f} + Ht + \text{const.}\end{aligned} \tag{25}$$

for constant of integration 'const.'

### 2.3 Evaluating the model

We consider a typical hierarchical triple system, of the sort that could be detectable with LISA. We take as our 'canonical' system, a triple with $m_0 = m_1 = 30M_\odot$, $m_2 = 10M_\odot$, orbital frequency $f = 10^{-3}$ Hz, $e_1 = 0.5$, $e_2 = 0.6$, and inclination $I = 60$ deg. We quantify the separation of the inner and outer binary via the parameter $\beta = a_2/a_1$ and set $\beta = 5$. The evolution of the orbital parameters as given by the analytical and numerical solutions is shown in Fig. 1 along with the relative error. The error in the analytical solution as compared to the numerical solution is of order of a few percent for $e(t)$ and $\gamma(t)$ and is $\sim 10^{-6}\%$ for $a(t)$.

### 2.4 Waveforms

With the orbital evolution specified, constructing the waveforms is straightforward. The two polarisations in the time domain for a Keplerian binary are given as the sum over the modes as,

$$h_+(t) = \sum_n (-1 + \cos^2 \iota) \left[a_n \cos 2\gamma - b_n \sin 2\gamma\right] + (1 - \cos^2 \iota) c_n \tag{26}$$

$$h_\times = \sum_n 2\cos\iota \left[a_n \sin 2\gamma + b_n \cos 2\gamma\right] \tag{27}$$

where,

$$a_n = -n\zeta[\bar{J}_{n-2}(ne) - 2e\bar{J}_{n-1}(ne) + \frac{2}{n}\bar{J}_n(ne) + 2eJ_{n+1} - J_{n+2}]\cos(n\Phi) \tag{28}$$

$$b_n = -n\zeta\sqrt{1-e^2}[\bar{J}_{n-2}(ne) - 2\bar{J}_n(ne) + \bar{J}_{n+2}(ne)]\ sin(n\Phi) \tag{29}$$

$$c_n = 2\zeta J_n(ne)\cos(n\Phi) \tag{30}$$

where $\bar{J}_n$ are Bessel functions of the first kind (as distinct from the angular momentum $J$) $\Phi$ is the mean anomaly and $\zeta = \mu(M\omega)^{2/3}/d$.

An example time-domain waveform for the canonical system is given in Fig 2. We can also compare this with the waveform in the case where we have switched off the Kozai couplings ($\dot{E}_{KL} = \dot{\gamma}_K L = 0$). As shown in Fig 3, whilst the waveforms are similar on shorter, orbital timescales, over longer timescales the waveforms exhibit marked differences.

In the same way that we evaluated the accuracy of our analytical solution to the orbital parameters, we want to see how faithfully

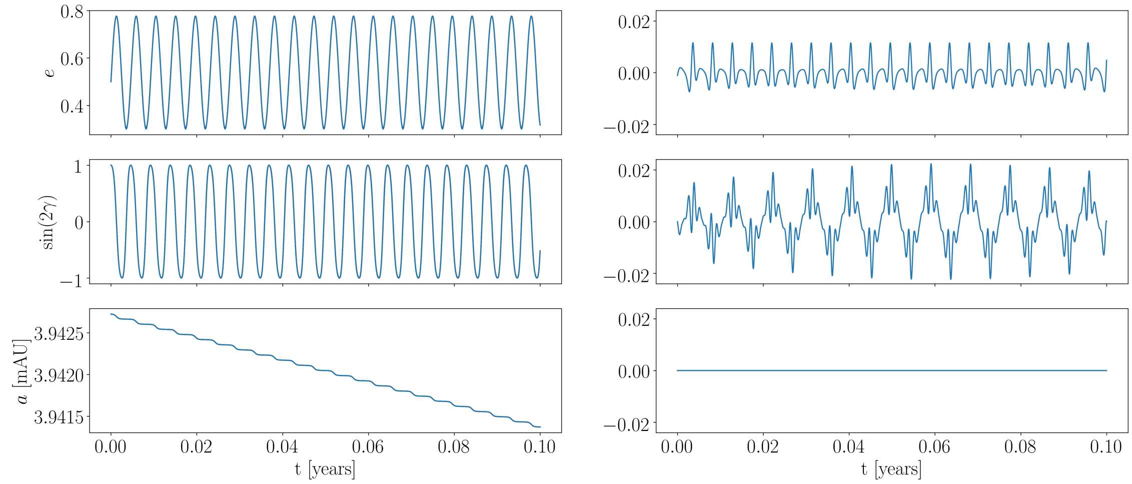


**Figure 1.** *Left column:* The time evolution of the orbital parameters as given by both the numerical solution and via our semi-analytical approximation. Both solutions are present but the difference cannot be resolved on this scale. *Right Column:* The relative error in the analytical solution as compared to the numerical one.

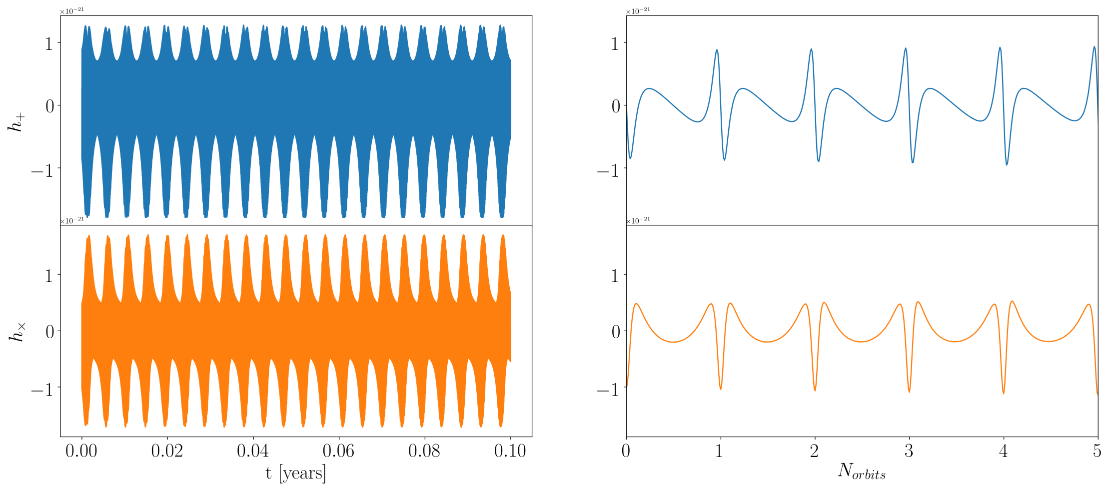


**Figure 2.** GW waveform in the time domain for our canonical system as given by the analytical solution. WE have set the observer at $\iota$ = 20 deg and the source at a distance of 1 Mpc, and performed a summation over 20 modes. The right-hand column shows the waveform over shorter (orbital) timescales

our model reproduces the gravitational waveforms. We define the overlap between two waveforms as,

$$\mathcal{O} = (\hat{a}|\hat{b}) \tag{31}$$

where $\hat{a}$ denotes a normalized unit vector such that

$$(\hat{a}|\hat{a}) = (\hat{b}|\hat{b}) = 1 \tag{32}$$

and $(\hat{a}|\hat{b})$ denotes an inner product defined with respect to the instrumental noise

$$(a|b) = 2\int^{\infty_0} \frac{\tilde{a}^*(f)\tilde{b}(f) + \tilde{b}^*(f)\tilde{a}(f)}{P_n(f)} df\,, \tag{33}$$

$f$ is the frequency and $P_n(f)$ is the noise power spectral density (PSD, Cutler & Flanagan 1994). For identical waveforms $\mathcal{O} = 1$ whilst completely anti-correlated signals have $\mathcal{O} = -1$ and $\mathcal{O} = 0$ for orthogonal signals. Each of the polarisations in the time domain can be transformed to the frequency domain via a Fourier transform,

$$\tilde{h}_{+,\times}(f) = \int_{-\infty}^{+\infty} h_{+,\times}(t)\exp(2\pi i f t) dt \tag{34}$$

The gravitational wave signal recorded by the detector is simply a linear combination of the two polarisation modes, corrected for the the response functions $F_{+,\times}$ of the LISA instrument,

$$\tilde{h}(f) = F_+(\Theta, \Phi, \Psi, f)\tilde{h}_+(f) + F_\times(\Theta, \Phi, \Psi, f)\tilde{h}_\times(f) \tag{35}$$

where $\Psi$ is the polarisation angle. Denoting the sky and polarisation

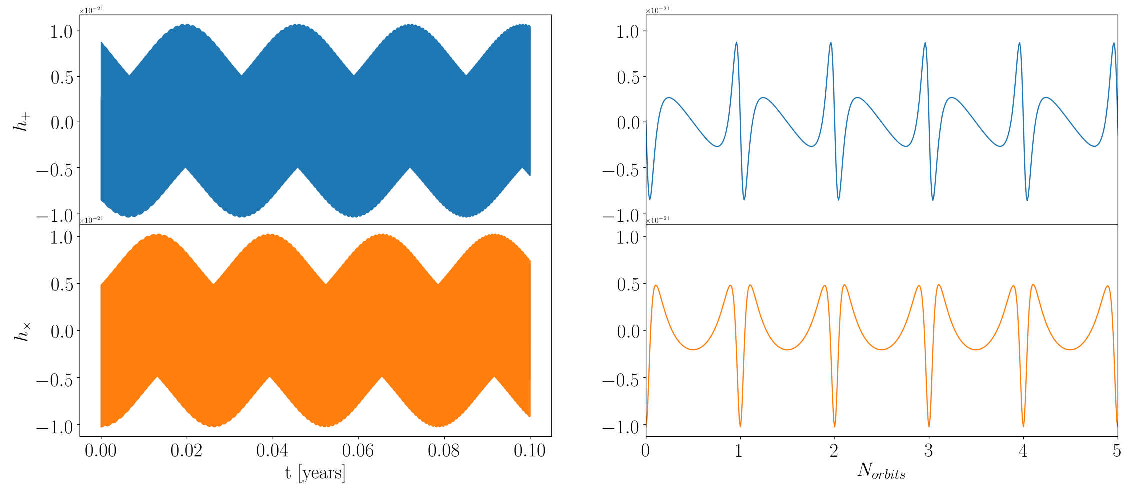


**Figure 3.** semi-analytical solution to the GW waveforms without Kozai effects

average as $\langle\rangle$, the averaged GW signal is given by

$$\langle \tilde{h}(f)\tilde{h}^*(f)\rangle = \mathcal{R}(f)\left(|\tilde{h}_+(f)|^2 + \tilde{h}_\times(f)|^2\right) \quad (36)$$

where $\mathcal{R}$ is the instrument response function averaged over the sky $(\Theta, \Phi)$ and polarization angle $(\Psi)$:

$$\mathcal{R}(f) = \langle F_+(f)F_+^*(f)\rangle = \langle F_\times(f)F_\times^*(f)\rangle \quad (37)$$

see Robson et al. (2019) for details. The overlap between the analytical and numerical solutions is then given as,

$$(a|b) = 2\int^{\infty 0} \frac{\tilde{a}_+(f)\tilde{b}_+(f) + \tilde{a}_\times(f)\tilde{b}_\times(f)}{S(f)} df \,, \quad (38)$$

where $S(f) = S_n(f) + S_c(f)$ and $S_n(f) = P_n(f)/\mathcal{R}(f)$ as defined in the subsequent section.

### 2.5 LISA Noise Model

The instrument response function does not have a closed form expression, but can be well fit as (Robson et al. 2019),

$$\mathcal{R}(f) = \frac{3}{10}\frac{1}{1 + 0.6(f/f_*)^2} \,, \quad (39)$$

and $f_*$ is the LISA transfer frequency. However, instead of this form we use the exact response function as given by **?**. The LISA noise PSD is given by

$$P_n(f) = \frac{P_{\rm OMS}}{L^2} + 2(1 + \cos^2(f/f_*))\frac{P_{\rm acc}}{(2\pi f)^4 L^2} \,, \quad (40)$$

for LISA arm length $L$. The optical metrology noise,

$$P_{\rm OMS} = (1.5 \times 10^{11}\ {\rm m})^2 \left(1 + \left(\frac{2\ {\rm mHz}}{f}\right)^4\right) {\rm Hz}^{-1} \,, \quad (41)$$

and the acceleration noise is,

$$P_{\rm acc} = (3 \times 10^{-15}\ {\rm m\ s}^{-2})^2 \left(1 + \left(\frac{0.4\ {\rm mHz}}{f}\right)^2\right) \left(1 + \left(\frac{f}{0.4\ {\rm mHz}}\right)^4\right) {\rm Hz}^{-1} \,. \quad (42)$$

| Parameter | Value |
|---|---|
| $\alpha$ | 0.1333 |
| $\beta$ | 243 |
| $\gamma$ | 917 |
| $\kappa$ | 482 |
| $f_k$ | 2.58 mHz |
| $A$ | $1.8 \times 10^{44}/N$ |
| $L$ | 2.5 Gm |
| $f_*$ | 19.09 mHz |

**Table 1.** Parameters for the noise model used in this work. We set the number of channels to be $N = 2$ and the transfer frequency is defined $f_* = c/(2\pi L)$

In addition to the instrumental noise, there is also an additional non-stationary noise contribution from the population of compact galactic binaries. This noise can be well described by the parametric function (**?**)

$$S_c(f) = Af^{-7/3}e^{-f^\alpha + \beta f \sinh(\kappa f)}\left[1 + \tanh(\gamma(f_k - f))\right] {\rm Hz}^{-1} \quad (43)$$

The fit parameters relevant for observation times greater than 4 years (i.e. bursting sources) are presented in Table 1 along with the fundamental LISA instrumental specifications. The characteristic strain is defined,

$$h_c^2 = f(S_n(f) + S_c(f)) \quad (44)$$

and the full LISA sensitivity curve in terms of this characteristic strain is presented in Fig. 4.

### 2.6 Overlaps

For our canonical system evaluated over 0.1 years at a sampling frequency of 0.1 Hz,the overlap is $\mathcal{O} = 0.9999648638407087$

## 3 CONCLUSION

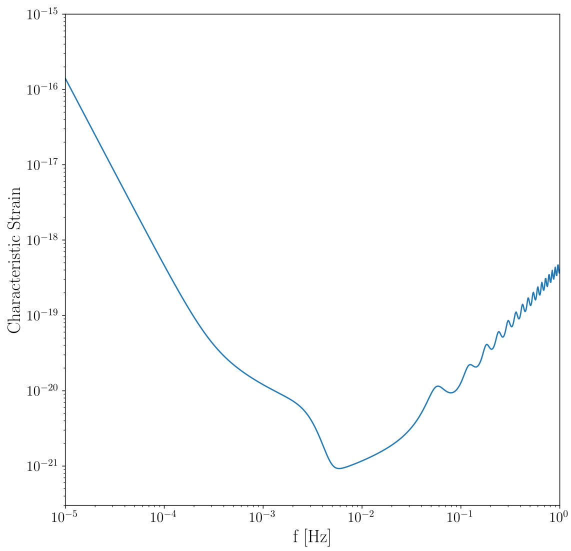


**Figure 4.** The LISA sensitivity curve. Characteristic strain is given by $\sqrt{f(S_n + S_c)}$

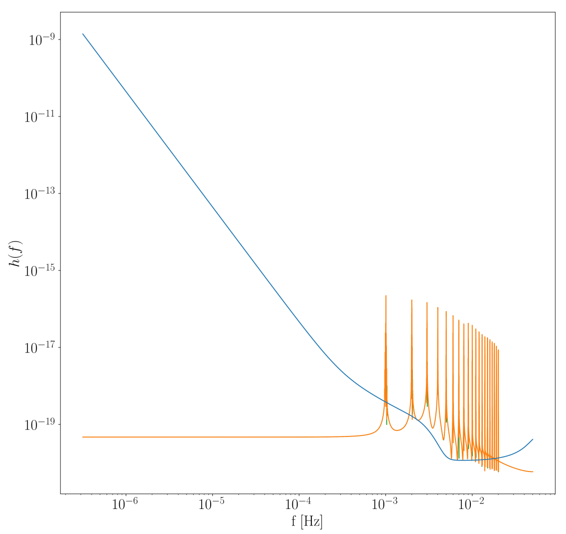


**Figure 5.**

## REFERENCES

Cutler C., Flanagan É. E., 1994, Phys. Rev. D, 49, 2658

Randall L., Xianyu Z.-Z., 2018, ApJ, 864, 134

Robson T., Cornish N. J., Liu C., 2019, Classical and Quantum Gravity, 36, 105011

This paper has been typeset from a TEX/LATEX file prepared by the author.